[Article ID] 1003- 6326(2001)05- 0748- 05

Pitting corrosion of Al2024-T3 in sodium chloride solution①

ZHANG Zhao(张 昭)[1], ZHANG Jian-qing(张鉴清)[1,2], SHAO Hai-bo(邵海波)[1], WANG Jian-ming(王建明)[1], CAO Chu-nan(曹楚南)[1,2]

(1. Department of Chemistry, Yuquan Campus, Zhejiang University, Hangzhou 310027, P. R. China; 2. State Key Laboratory for Corrosion and Protection, Shenyang 110015, P. R. China)

[Abstract] Pitting corrosion behavior of Al2024-T3 in sodium chloride solution was investigated by using potentiodynamic scanning (PDS) measurements and electrochemical impedance spectroscopy (EIS) technique. When pitting corrosion of the alloy occurs, there exists a passive region in the anodic branch of PDS polarization curve, which is enlarged with the increasing of immersion time due to the competition of the halide ions with OH^- ions to adsorb on the oxide film to form the corrosion products film and the increase of pitting corrosion area. Two capacitive semicircles were observed in complex plane plot. For more extensive pitting and general corrosion of Al2024-T3, the passive region in PDS disappeared, while another depressed semicircle was observed in Nyquist plot because of the formation of corrosion products film. On the other hand, the low frequency inductive loop, which had often been regarded as a manifestation of pitting or formation and precipitation of a salt film, was not observed, which indicates that the low frequency inductive loop can not be the characteristic of pitting corrosion or the formation of salt film. The results also show that higher reactant CPE exponent values will correspond to more extensive transformation of a metal surface by very localized corrosion, while general corrosion can result in a smaller CPE exponent value.

[Key words] Al2024-T3; pitting corrosion; electrochemical impedance spectroscopy; potentiodynamic scanning

[CLC number] TG 174.3; O 646 [Document code] A

1 INTRODUCTION

Aluminum and its alloys are widely used in the telecommunications, electronics and aviation industries because of their good electrical conductivity and processability. But they are very susceptible to pitting corrosion in aqueous environments, and the pitting corrosion process can be accelerated by combined presence of reactive anions in solution and some intermetallic inclusions embedded in the metal matrix[1~6].

It is well known that pitting corrosion process consists of three stages: initiation, propagation and repassivation. The pit propagation stage can be further divided into three steps defined by the rate-controlling process[7,8]: 1) As soon as a pit is nucleated, the dissolution of matrix metal becomes the rate controlling step, duration of which is short because the saturation of the pit environment is quickly achieved. The step is often characterized by the formation of a nonprotective salt film composed of the dissolved metal cations and concentrated aggressive anions with high ionic conductivity at the inner surface of the pit. 2) The nonprotective salt film provides a high capacity for the dissolution of the metal, which leads the ion migration process to be the rate controlling step. The ion migration process, which constitutes most of the lifetime of a pit growth is produced by diffusion and electromigration under the concentration gradient and the potential gradient in the pit. In addition, the dissolved metal cations undergo hydrolysis reactions, resulting in an autocatalytic condition. 3) When the potential drop inside the pit or the potential of the dissolved metal decreases, the metal dissolution capacity of the inner metal surface also decreases, while the rate of formation of nonprotective film (hydrous product of metal and aggressive anions) increases. Therefore, the pit growth process terminates, and the repassivation of a pit begins.

Traditionally, pitting potential (φ_p) and protection or repassivation potential (φ_{pr}) are used to characterize the material's resistance against pitting, where φ_p is related to the pit initiation and φ_{pr} is proposed to be associated with pit growth. Smaller difference ($\varphi_p - \varphi_{pr}$), as determined from potentiodynamic scanning (PDS) or cyclic polarization (CP), indicates greater resistance to pit growth[9~11]. However, the values of them are governed by a number of factors, such as the environment and the scan rate used in the measurement[9]. On the other hand, the mechanism of pitting corrosion is still not very clarified, and some doubts remain for further investigation. Meanwhile, pitting corrosion can lead to the premature failure of high-strength Al alloys used in aerospace structures and lose their promising characteristics as engineering materials for many other industrial applications. Hence, a better understanding of their pitting corrosion behavior is of scientific inter-

① [Foundation item] Project (G1990650) supported by the National Key Basic Research Foundation of China; Project (50071054) supported by the National Natural Science Foundation of China [Received date] 2000- 10- 30; [Accepted date] 2001- 02- 22

est and technological importance.

The authors intend to study the corrosion behavior of Al 2024-T3 in sodium chloride solution by means of potentiodynamic measurements and electrochemical impedance spectroscopy (EIS) and to develop an appropriate model for the impedance, from which the parameters characterizing the corrosion process can be extracted.

2 EXPERIMENTAL

Specimens of 2 cm in length were cut from commercial aluminum rod of 28.26 mm in diameter, with the chemical composition (mass fraction, %): 4.24 Cu, 1.26 Mg, 0.65 Mn, 0.15 Fe, 0.06 Si, 0.08 Zn, 0.031 Ti, < 0.01Cr, and balance Al. The specimens were connected respectively to a copper wire using screw at one cross section to accommodate the specimen and provide electrical contact, then mounted in epoxy with the other cross section exposed. Before testing, the exposed surface was polished using abrasive papers through 500-grade to 1200-grade, then rinsed using distilled water, degreased using acetone and ethanol and dried for 30 min in air.

Electrochemical measurements were carried out in a three-compartment cell. The working electrode was the Al 2024-T3, a large platinum sheet and a saturated calomel electrode (SCE) with a Luggin capillary served as counter and reference electrodes respectively. Both were separated from the main compartment of the cell by fine-pored glass diaphragms. All potentials were referred to the SCE. All tests were carried out in 2% neutral sodium chloride solution (1.5 L) prepared using analytical reagents and deionized water at ambient temperature.

Electrochemical impedance spectroscopy (EIS) measurements were performed with a commercial electrochemical analyzer/workstation (Model 660A) at the open circuit potential. EIS was always taken in the direction of decreasing frequency and each EIS measurement was repeated five times in order to ascertain the stability of the system being evaluated. A frequency range of 10^5 Hz to 0.015 Hz was selected for its sensitivity to corrosion resistance. The alternating current was applied directly between the working electrode and the counter electrode, and kept at a value which would not cause more than 5 mV difference (peak to peak) across the cell to maintain the linear relationship between the applied potential and the response current. During the experiments, the specimens were examined with optical microscopy to observe the change in corrosion morphologies.

3 RESULTS AND DISCUSSION

3.1 Potentiodynamic measurement

Fig. 1 represents the potentiodynamic scanning

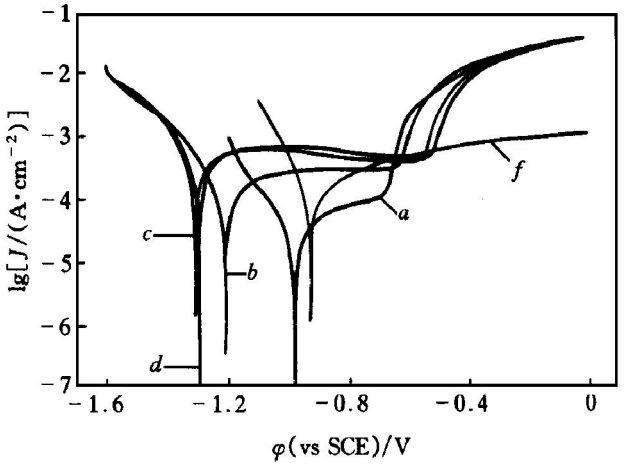

Fig. 1 Potentiodynamic plots for Al2024-T3 in 2.0% neutral NaCl solution at different immersion time

Curve *a* —40 min; Curve *b* —198 min; Curve *c* —1 495 min; Curve *d* —2 835 min; Curve *f* —4 320 min

(PDS) curves of Al2024-T3 in 2.0% neutral sodium chloride solution at a sweep rate of 0.01 V/s, between − 200 mV to − 250 mV from open circuit potential (OCP) and + 1 000 mV from OCP. Before pitting corrosion begins (curves a ~ d), there exists a distinct passive region ($\Delta\varphi$) between the primary passivation potential (φ_{pr}) and the oxide film breakdown potential (φ_p), the value, $\Delta\varphi(=\varphi_p-\varphi_{pr})$, increases with the immersion time while the current density in this region increases with time, which may be attributed to the competition of the halide ions with OH^- ions to adsorb on the oxide film to form $Al(OH)_{p-m}Cl_m$[7,8] and the increase in pitting corrosion area.

Pitting corrosion of Al2024-T3 proceeds according to the following reactions:

$$\gamma\text{-}Al_2O_3\cdot H_2O \rightleftharpoons \alpha\text{-}Al(OH)_p \quad (1)$$

$$\alpha\text{-}Al(OH)_p + m\,Cl^- \rightleftharpoons Al(OH)_{p-m}Cl_m + m\,OH^- \quad (2)$$

Therefore, when the applied potential becomes more positive than OCP and increases positively, the anodic current is controlled by two factors: 1) diffusion of halide ions from solution to the interface of oxide film and counter diffusion of OH^- ions, and 2) chemical reaction rate of reactions (1) and (2). Consequently, the above factors result in the enlargement of passive region and anodic current density.

After a long time of corrosion of Al2024-T3 (curve *f*), passive region disappears in the anodic branches of PDS curves and no φ_p and φ_{pr} potentials appear to be present, the current continues increasing with potential throughout the entire forward anodic potential scan. The reason for these phenomena is that the oxide film on the Al2024-T3 surface has mostly transformed into $Al(Cl)_n$[7,8], which is soluble in the solution. Meanwhile, some corrosion black

products cover the entire surface of the material in the general and pitting corrosion, are expected to occur.

3.2 AC impedance measurement

The equivalent circuit (EC), shown in Fig. 2, was utilized with the Boukamp program to simulate the impedance characteristics of Al2024-T3 in NaCl solution at rest potential. Within the passive region, two capacitive semicircle can be resolved in complex plane plot when the high frequency behavior is enlarged (Figs. 3 and 4). The semicircle at the highest frequency with shorter time constant probably arises from the dielectric property of the surface film, and the second depressed ($\lg(Z)/\lg(f) < 0.1$) capacitive semicircle is associated with the oxide film formed on the Al2024-T3 surface, the diameter of semicircle decreases with the prolonging of immersion time due to the thinning of the original oxide film.

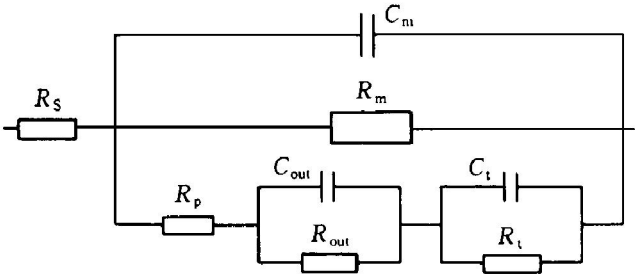

Fig. 2 Equivalent circuit for Al2024-T3 in neutral NaCl solution

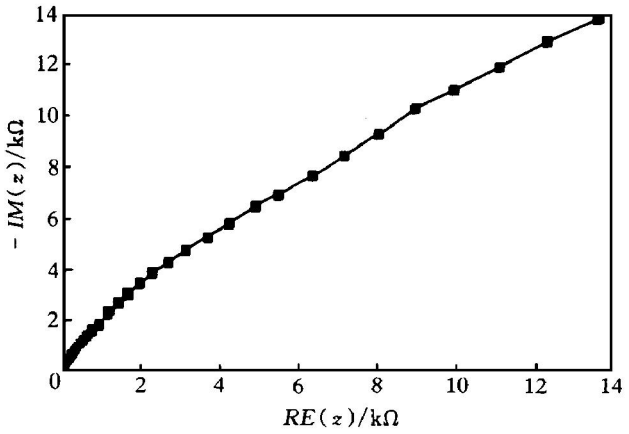

Fig. 3 Nyquist plot for duration time of pitting corrosion of Al2024-T3 in NaCl solution

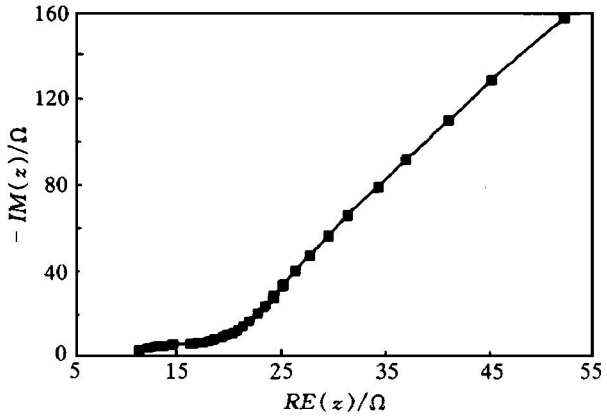

Fig. 4 Enlarged diagram in high frequency range of plot in Fig. 3

In some cases, simulation of the impedance spectra can be improved by replacing the capacitance, C, with a constant phase element, $CPE = 1/Y_0(j\omega)^n$, which is expressed as an exponent affecting the imaginary component of a complex impedance. For $n = 1$, CPE represents an ideal capacitance with $C = Y_0$; $n = 0$ a resistance with $R = Y_0^{-1}$; $n = 0.5$, a warburg; and $n = -1$, an inductance with $L = Y_0^{-1}$. The presence of a CPE often has been explained by dispersion effects that might be caused by microscopic roughening of a surface[12~14], which, in turn, have been related to surface preparation or localized corrosion[15, 16].

In our experiments, the reactant CPE (Q_t) exponents (n) were close to one (approximately 0.9) at the beginning of immersion time decreasing with the time of immersion. It is shown that higher reactant CPE exponent values would correspond to more extensive transformation of a metal surface by very localized corrosion, while smaller CPE exponent value would correspond to general corrosion[17]. The reactant resistance (R_t) and other equivalent elements' values after immersion for different time, obtained using Boukamp program, are listed in Table 1. As expected, the reactant resistance decreased with time, caused by the breakdown of the oxide film and the increase of electro-dissolution rate, indicating an increase of corrosion rate with immersion time, while the pore resistance R_p and corrosion product resis-

Table 1 R_t, R_p and other fitted values of elements of equivalent circuit

Immersion time/min	R_s / Ω	Q_m Y_0/ Ωs	Q_m n	R_m / Ω	R_p / Ω	R_{out} / Ω	Q_{out} Y_0/ Ωs	Q_{out} n	R_t / Ω	Q_t Y_0/ Ωs	Q_t n
38	3.44	4.988×10^{-5}	0.43	4.80×10^{19}	12.65	8.67	1.998×10^{-6}	0.99	4.81×10^{19}	1.11×10^{-5}	0.93
240	4.82	5.24×10^{-5}	0.42	4.20×10^{4}	12.38	7.30	1.08×10^{-5}	0.87	4.41×10^{4}	2.79×10^{-5}	0.91
1 220	9.30	2.49×10^{-6}	0.85	2.73×10^{19}	17.43	81.87	8.12×10^{-4}	0.60	6.95×10^{3}	1.06×10^{-4}	0.93
3 760	5.12	1.40×10^{-7}	1	3.73×10^{19}	23	2.02×10^{3}	7.79×10^{-3}	1	4.16×10^{3}	1.11×10^{-4}	0.73

tance R_{out} increase, caused by the formation of product film on the surface of the corroding electrode. The film resistance R_m decreases at first because of the thinning of the oxide film, then increases due to the formation of corrosion products film.

For more extensive pitting of 2024-T3 (longer duration and/or greater anodic polarization), the surface of the corroding electrode was covered by a layer of clearly evident black salt film containing pits. Another capacitive semicircle in the low frequency region was observed. Its diameter increases with the immersion time. This was assumed to be related to the formation of a thick but nonprotective composite layer of oxides and corrosion products, and hence, to the corroding intensity (Figs. 5 and 6). With the increasing immersion time, the low frequency capacitive semicircle was found to become dominating by diffusion processes (Fig. 5). On the other hand, no low frequency inductive loop, which has been interpreted as a manifestation of pitting by Metikos-Hunkovic and Bessone et al[18], or has been regarded to be associated with the formation and precipitation of a salt film by Breslin and Rudd[19], was observed. This implies that the low frequency inductive loop may not be the characteristic of pitting corrosion or the formation of salt film.

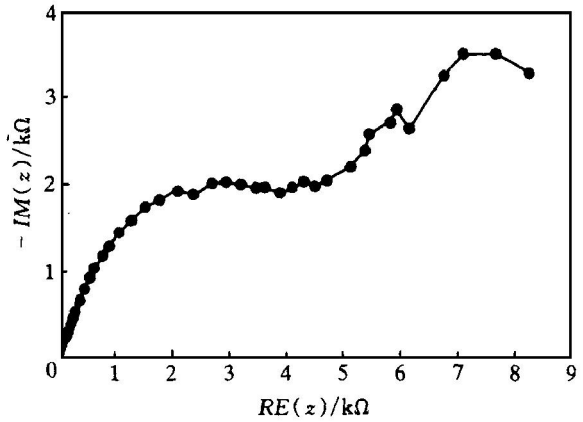

Fig. 5 Complex plane impedance plot for more extensive pitting corrosion of Al2024-T3 in NaCl solution

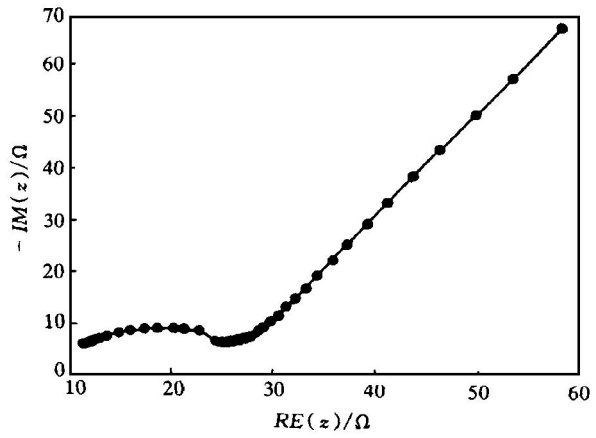

Fig. 6 Enlarged diagram in high frequency range of diagram in Fig. 5

4 CONCLUSIONS

During pitting corrosion of aluminum alloy, 2024-T3 in neutral sodium chloride solution, in PDS plot there exists a passive region, which expands with the immersion time. This phenomenon may be attributed to the competition of the chloride ions with OH^- ions to adsorb on the oxide film to form the corrosion products $Al(OH)_{p-m}Cl_m$ and the increase of pitting corrosion area. Once general corrosion occurs, the passive region disappears. Meanwhile, two depressed semicircles can be observed in Nyquist plot within the passive region, the high frequency semicircle was regarded to be related to the dielectric performance of the surface film, while the other may be associated with the oxide film on the Al2024-T3 surface, the diameter of semicircle decreases with the immersion time due to the thinning of the oxide film. The second depressed semicircle appears with the prolongation of immersion time due to the formation of corrosion products film, and its diameter increases with the immersion time. However, no low frequency inductive loop was observed. It implies that the low frequency inductive loop is not the characteristic of pitting corrosion or the formation of salt film.

ACKNOWLEDGEMENTS

The authors wish to acknowledge the financial support of the State Key Laboratory for Corrosion and Protection (China).

[REFERENCES]

[1] Liao C M, Olive J M, Gao M, et al. In-situ monitoring of pitting corrosion in aluminum alloy 2024 [J]. Corrosion, 1998, 54(6): 451-458.

[2] Chen G S, Gao M, Wei R P. Microconstituent-induced pitting corrosion in aluminum alloy 2024-T3 [J]. Corrosion, 1996, 52(1): 8-15.

[3] Salinas D R, Bessone J B. Electrochemical behavior of Al-5%Zn-0.1%Sn sacrificial anode in aggressive media: influence of its alloying elements and the solidification structure [J]. Corrosion, 1991, 47(9): 665-674.

[4] Latanision R M. Corrosion science, corrosion engineering and advanced technologies [J]. Corrosion, 1995, 51(4): 270-283.

[5] Brusic V, Frankel G S, Hu C K, et al. Corrosion study of an Al-Cu alloy exposed to reactive ion etching [J]. Corrosion, 1991, 47(1): 35-40.

[6] Buchheit R G Jr, Moran J P, Stoner G E. Localized corrosion behavior of alloy 2090: the role of microstructural heterogeneity [J]. Corrosion, 1990, 46(8): 610-617.

[7] Graedel T E. Corrosion mechanisms for aluminum exposed to the atmosphere [J]. J Electrochem Soc, 1989,

136(4): 204C- 212C.

[8] Foley R T. Localized corrosion of aluminum alloys: a review [J]. Corrosion, 1986, 42(5): 278- 288.

[9] Choi D, Was G S. Development of a pit growth resistance parameter for the study of pit growth in alloy 600 [J]. Corrosion, 1992, 48(4): 292- 305.

[10] Hunkeler F, Frankel G S, Bohni H. On the mechanism of localized corrosion [J]. Corrosion, 1987, 43(3): 189- 191.

[11] Lyberatos G, Kobotiatis L. Inhibition of aluminum 7075 alloy corrosion by the concerted action of nitrate and oxalate salts [J]. Corrosion, 1991, 47(11): 820- 824.

[12] Cole K S, Cole R H. Dispersion and adsorption in dielectrics (part one): alternating current characteristics [J]. J Chem Phys, 1941, 9: 341- 351.

[13] Davidsont D W, Cole R H. Dielectric relaxation in glycerol, propylene glycol, and *n*-propanol [J]. J Chem Phys, 1951, 19: 1484- 1490.

[14] de Levie R. The influence of surface roughness of solid electrodes on electrochemical measurements [J]. Electrochimica Acta, 1965, 10: 113- 130.

[15] Roberge P R, Halliop E, Asplund M, et al. Electrochemical impedance spectroscopy as a valuable monitoring technique for various forms of corrosion [J]. J Appl Electrochem, 1990, 20: 1004- 1008.

[16] Roberge P R, Halliop E, Sastri V S. Corrosion of mild steel using electrochemical impedance spectroscopy data analysis [J]. Corrosion, 1992, 48(6): 447- 454.

[17] Roberge P R, Sastri V S. On line corrosion monitoring with electrochemical impedance spectroscopy [J]. Corrosion, 1994, 50(10): 744- 754.

[18] Metikos-Hunkovic M, Barbic R, Grubac Z, et al. Impedance spectroscopic study of aluminum and Al-al-loys in acid solution: inhibitory action of nitrogen containing compounds [J]. J Appl Electrochem, 1994, 24: 772- 778.

[19] Breslin C B, Rudd A L. Activation of pure Al in an indium-containing electrolyte—an electrochemical noise and impedance study [J]. Corros Sci, 2000, 42: 1023 - 1039.

(Edited by HE Xue-feng)